Proc. NIPR Symp. Polar Meteorol. Glaciol., **11**, 178-198, 1997

STRATOSPHERIC SUDDEN WARMING IN 1989 FROM THE VIEWPOINT OF ATMOSPHERIC ANGULAR MOMENTUM

Dong-Il SEOL and Koji YAMAZAKI

Hokkaido University, Kita-10, Nishi-5, Kita-ku, Sapporo 060

Abstract: A major wavenumber-2 stratospheric sudden warming occurred in mid-February of 1989. Using the U.S. National Meteorological Center (NMC) data, an analysis of this event was performed based on the angular momentum equation in the transformed Eulerian-mean (TEM) formalism. Although the warming took place abruptly, the atmospheric angular momentum (AAM) of the Northern Hemisphere (NH) stratosphere above 100 hPa started decreasing gently about 4 weeks before the warming. The decreasing occurred in the whole region of the NH stratosphere. During the decreasing period of the northern stratospheric AAM prior to the sudden warming, the global AAM also decreased and hence the length of day (LOD) decreased. The contribution of the global stratospheric AAM to the decreasing of the LOD was about 40-50%. Using the TEM formalism, the AAM budget in the NH stratosphere was investigated. The eddy forcing which can be represented as the Eliassen-Palm (E-P) flux vectors generally acts to decrease the AAM, and the residual mean meridional circulation acts in the opposite way. Analysis of the relationship between the stratospheric sudden warming and the AAM budget shows that the eddy forcing was enhanced gradually during the 4 weeks before the warming and contributed to the decreasing of the AAM.

1. Introduction

The atmospheric angular momentum (AAM), which reflects the distribution of the zonal winds in the atmospheric circulation, plays an important role in changes of the length of day (LOD). The variations in the globally integrated AAM are well correlated with changes of a few tenths of a millisecond in the LOD and can account for changes of the LOD of period less than several years (LANGLEY *et al.*, 1981; EUBANKS *et al.*, 1985; NAITO, 1988; NAITO and KIKUCHI, 1992b). Therefore, the changes of the LOD are a good indicator of climate variability (ONODERA and NAITO, 1987). For example, the signals of the El Niño-Southern Oscillation, Quasi-Biennial Oscillation, and 40- to 50-day oscillation appear in the LOD (ROSEN *et al.*, 1984; CHAO, 1989; NAITO and KIKUCHI, 1992a; MAGAÑa, 1993).

ROSEN and SALSTEIN (1985) and JADIN and YAMAZAKI (1995) have studied the contribution of stratospheric winds to annual and semiannual fluctuations in AAM and the LOD. They showed that including stratospheric winds in the AAM calculation reduced significantly the differences of the amplitudes of annual and semiannual components between the globally integrated tropospheric AAM and LOD. In general, the climatological zonal-mean zonal winds are westerly in the winter stratosphere. Strato-

spheric sudden warming is a dramatic event which decreases rapidly the westerlies in the high-latitude stratosphere and increases the westerlies in low-latitudes of the stratosphere. The net effect for the stratospheric AAM in connection with this event is not clear.

Stratospheric sudden warming has been studied from various points of view for 40 years or more. However, warming events have not been studied from the viewpoint of the AAM and LOD. A major wavenumber-2 stratospheric sudden warming occurred in mid-February of 1989. In this study, we examine the relationships between the stratospheric sudden warming and the AAM, LOD variations for this case. To investigate the AAM budget in the Northern Hemisphere (NH) stratosphere in connection with the stratospheric sudden warming, we use the angular momentum equation in the transformed Eulerian-mean (TEM) formalism.

This paper is organized as follows. In Section 2, the data and method of analysis are described. Section 3 contains a description of the behavior of the major warming. In Section 4, the relationships between the stratospheric sudden warming and the AAM, LOD variations are shown. Quantitative results for the AAM budget in the NH stratosphere are shown in Section 5. Finally, the results are summarized and discussed in Section 6.

2. Data and Method of Analysis

In this study, we used the U.S. National Meteorological Center (NMC, presently known as the National Centers for Environmental Prediction (NCEP)) 1200 GMT daily data during the period from January to March 1989. Geopotential heights and temperatures are available on a $2.5^\circ \times 5.0^\circ$ latitude-longitude grid at 18 pressure levels (1000, 850, 700, 500, 400, 300, 250, 200, 150, 100, 70, 50, 30, 10, 5, 2, 1, and 0.4 hPa). Winds are available from 1000 hPa to 50 hPa level. Above 50 hPa, the nonlinear balance wind was computed from the geopotential height data between 20° latitude and 90° latitude (RANDEL, 1987). Between 10° latitude and 20° latitude, a linear combination of the geostrophic wind and the nonlinear balance wind was used. The wind near the equator was obtained by cubic-spline interpolation from the values at 10°N/S and poleward of them. Missing data were linearly interpolated in time.

LOD data used in this study are synthetic data observed astronomically by space techniques: *i.e.*, lunar laser ranging (LLR), satellite laser ranging (SLR), and very long baseline interferometry (VLBI) (GROSS, 1992, data are provided by Dr. I. NAITO).

The AAM relative to an earth-fixed frame for various latitudinal belts is computed by

$$AAM = \frac{2\pi a^3}{g} \int_{p_s}^{p_t} \int_b \bar{u} \cos^2 \phi \, d\phi dp, \tag{1}$$

where ϕ ranges between the southern and northern boundaries of belt b. Here a is the mean radius of the Earth, g is the acceleration due to gravity, ϕ is latitude, $\bar{u}$ is the zonal-mean zonal wind, p_s is the surface pressure (here we assume 1000 hPa as p_s), and p_t is the top pressure of the atmosphere.

On the one hand, the angular momentum equation in the TEM formalism can be written (*e.g.*, HOLTON *et al.*, 1995)

$$\frac{\partial \overline{m}}{\partial t} + \frac{\overline{v}^*}{a} \frac{\partial \overline{m}}{\partial \phi} + \overline{w}^* \frac{\partial \overline{m}}{\partial z} = (a \cos\phi) \overline{G}. \tag{2}$$

Here $\overline{m}=a\cos\phi(\overline{u}+a\Omega\cos\phi)$ is the absolute angular momentum, $\overline{G}$ represents the wave-induced force per unit mass, overbars denote zonal means, $z=-H\ln(p/p_s)$ where H is a scale height (7 km), and Ω is the angular velocity of the Earth. In the TEM formalism (*e.g.*, ANDREWS and MCINTYRE, 1976; EDMON *et al.*, 1980; PALMER, 1981), a residual mean meridional circulation is defined by

$$\overline{v}^*=\overline{v}-\frac{1}{\rho_0}\frac{\partial}{\partial z}(\rho_0\overline{v'\theta'}/\overline{\theta}_z), \tag{3}$$

$$\overline{w}^*=\overline{w}+\frac{1}{a\cos\phi}\frac{\partial}{\partial\phi}(\cos\phi\overline{v'\theta'}/\overline{\theta}_z). \tag{4}$$

Here subscripts such as z in $\overline{\theta}_z$ represent partial differentiation, primes denote departures from zonal means, $\rho_0(z)=\rho_s e^{-z/H}$ where $\rho_s=p_s/RT_s$, R is the gas constant, T_s is a constant reference temperature (239.2 K), and θ is the potential temperature.

Integrating eq. (2) over altitudinal and latitudinal volume $(z_1-\infty,\ \phi_1-\phi_2)$ for the volume element for integrating over a zonally symmetric portion of the atmosphere, $2\pi a^2\cos\phi\ d\phi dz$ and making $\phi_2\to\frac{\pi}{2}$ (90°N), the first term on the left-hand side of eq. (2) can be written

$$\begin{aligned}\frac{\partial M}{\partial t}&=\frac{\partial}{\partial t}\left\{2\pi a^2\int_{z_1}^{\infty}\int_{\phi_1}^{\frac{\pi}{2}}\rho_0\cos\phi\ \overline{m}\ d\phi dz\right\}\\&=\frac{\partial}{\partial t}\left\{2\pi a^3\int_{z_1}^{\infty}\int_{\phi_1}^{\frac{\pi}{2}}\rho_0\cos^2\phi\overline{u}\,d\phi dz+2\pi a^4\Omega\int_{z_1}^{\infty}\int_{\phi_1}^{\frac{\pi}{2}}\rho_0\cos^3\phi\ d\phi dz\right\}\\&=\frac{\partial M_r}{\partial t}+\frac{\partial M_\Omega}{\partial t},\end{aligned} \tag{5}$$

where

$$M_r=2\pi a^3\int_{z_1}^{\infty}\int_{\phi_1}^{\frac{\pi}{2}}\rho_0\cos^2\phi\overline{u}\,d\phi dz,$$

$$M_\Omega=2\pi a^4\Omega\int_{z_1}^{\infty}\int_{\phi_1}^{\frac{\pi}{2}}\rho_0\cos^3\phi\ d\phi dz.$$

In eq. (5), M_r represents the relative angular momentum, which we already discussed in eq. (1). M_Ω is called Ω momentum and represents the angular momentum of the atmosphere if it were at rest with respect to the rotating solid Earth. M_Ω is almost constant with time. Since the time-variation of M_Ω is much smaller than that of M_r, we neglect the time-variation of M_Ω in this study. Using the continuity equation, the second and third terms on the left-hand side of eq. (2) can be written in flux form:

$$\frac{1}{a\cos\phi}\frac{\partial}{\partial\phi}(\cos\phi\overline{v}^*\overline{m})+\frac{1}{\rho_0}\frac{\partial}{\partial z}(\rho_0\overline{w}^*\overline{m}).$$

Integrating over the same volume, we obtain:

$$\begin{aligned}&2\pi a\int_{z_1}^{\infty}\int_{\phi_1}^{\frac{\pi}{2}}\rho_0\frac{\partial}{\partial\phi}(\cos\phi\overline{v}^*\overline{m})\ d\phi dz+2\pi a^2\int_{\phi_1}^{\frac{\pi}{2}}\int_{z_1}^{\infty}\cos\phi\frac{\partial}{\partial z}(\rho_0\overline{w}^*\overline{m})\ dzd\phi\\&=-2\pi a\cos\phi_1\int_{z_1}^{\infty}\rho_0\overline{v}^*(\phi_1)\overline{m}(\phi_1)\ dz-2\pi a^2\int_{\phi_1}^{\frac{\pi}{2}}\cos\phi\rho_0(z_1)\overline{w}^*(z_1)\overline{m}(z_1)\ d\phi.\end{aligned} \tag{6}$$

The wave-induced force $\overline{G}$ on the right-hand side of eq. (2) can be written:

$$\overline{G}=\frac{1}{\rho_0 a\cos\phi}\nabla\cdot\mathbf{F}+\overline{X}. \tag{7}$$

Here $\overline{X}$ represents the unspecified horizontal components of friction, or other nonconservative mechanical forcing. $\mathbf{F}$ is the Eliassen-Palm (E-P) flux owing to eddies such as planetary waves. E-P flux vectors in the TEM formalism are defined by

$$\boldsymbol{F}^{(\phi)}=\rho_0 a\cos\phi(\bar{u}_z\,\overline{v'\theta'}/\bar{\theta}_z-\overline{v'u'}), \tag{8}$$

$$\boldsymbol{F}^{(z)}=\rho_0 a\cos\phi\left\{\left[f-\frac{1}{a\cos\phi}\frac{\partial}{\partial\phi}(\bar{u}\cos\phi)\right]\overline{v'\theta'}/\bar{\theta}_z-\overline{w'u'}\right\}, \tag{9}$$

and $\nabla\cdot\mathbf{F}$ is expressed by

$$\nabla\cdot\mathbf{F}=\frac{1}{a\cos\phi}\frac{\partial}{\partial\phi}(\boldsymbol{F}^{(\phi)}\cos\phi)+\frac{\partial\boldsymbol{F}^{(z)}}{\partial z}. \tag{10}$$

If we neglect $\overline{X}$, the right-hand side of eq. (2) can be written

$$\begin{aligned}&2\pi a^2\int_{z_1}^{\infty}\int_{\phi_1}^{\frac{\pi}{2}}\rho_0\cos\phi(a\cos\phi)\overline{G}\;d\phi dz\\&=-2\pi a\cos\phi_1\int_{z_1}^{\infty}\boldsymbol{F}^{(\phi)}(\phi_1)\;dz-2\pi a^2\int_{\phi_1}^{\frac{\pi}{2}}\cos\phi\boldsymbol{F}^{(z)}(z_1)\;d\phi.\end{aligned} \tag{11}$$

From eqs. (5), (6), and (11), the time-variation of the AAM is given by

$$\begin{aligned}\frac{\partial M}{\partial t}=\frac{\partial M_r}{\partial t}&=2\pi a\cos\phi_1\int_{z_1}^{\infty}\rho_0\overline{v}^*(\phi_1)\overline{m}(\phi_1)\;dz\\&+2\pi a^2\int_{\phi_1}^{\frac{\pi}{2}}\cos\phi\rho_0(z_1)\overline{w}^*(z_1)\overline{m}(z_1)\;d\phi\\&-2\pi a\cos\phi_1\int_{z_1}^{\infty}\boldsymbol{F}^{(\phi)}(\phi_1)\;dz\\&-2\pi a^2\int_{\phi_1}^{\frac{\pi}{2}}\cos\phi\boldsymbol{F}^{(z)}(z_1)\;d\phi.\end{aligned} \tag{12}$$

Equation (12) suggests that the time-variation of the AAM can be calculated from the meridional and vertical components of the residual mean meridional circulation and E-P flux vectors; therefore, using this equation, we can examine the AAM budget and causes of the AAM variation in a certain region and time. The analysis which is related to eq. (12) is described in Section 5.

3. Behavior of the Major Warming

Stratospheric sudden warmings can be mainly divided into major warmings and minor warmings. It is defined to be a major warming if at 10 hPa or below the zonal-mean temperature increases poleward from 60° latitude and the zonal-mean zonal wind reverses in a period of a week or less. If the temperature gradient reverses there but the circulation does not, it is defined to be a minor warming (ANDREWS *et al.*, 1987).

We survey the behavior of the major warming which occurred in mid-February of 1989 before analyzing the relationship between the stratospheric sudden warming and the

AAM variation. Subsection 3.1 shows a description of the zonal-mean and synoptic fields at the time of the major warming. The E-P flux vectors and the residual mean meridional circulation which are useful concepts in the diagnosis of the stratospheric sudden warming and the time-variation of the AAM are described in Subsection 3.2.

3.1. Zonal-mean and synoptic fields

Figure 1 shows the time evolution of temperature at 10 hPa and 30 hPa over the North Pole. During January and February of 1989, three sudden warming events (around January 26–29, February 9–12, and February 15–20) occurred in the northern polar stratosphere. While the third event showed the strongest warming at 30 hPa, as much as 41.4 K from February 15 to February 20, the first two of these events took place at higher levels than the third event. The third event was more rapid and stronger than the others. In all events, the zonal-mean temperatures increased poleward from 60°N at 10 hPa or below (not shown).

Figure 2 shows the latitude-height sections of the zonal-mean zonal wind during the third event, which is the strongest warming among the three sudden warming events. Figure 3 shows the change of the zonal-mean zonal wind for two days during that period. On February 14, the stratospheric westerly jet was located at around 70°N, 10 hPa and had a maximum around 45–50 ms^{-1}. The westerly jet was weakened in connection with the sudden warming (Figs. 2b, 2c, 3b, and 3c), and the easterly appeared from the high-latitude upper stratosphere as the warming progressed (Fig. 2c). In the latter half of the warmimg, whereas the stratospheric circulation in high-latitudes reversed to easterly, the westerly in the low-latitude upper stratosphere became strong at a slow pace (Figs. 2d, 2e, 3d, and 3e). The maximum of the easterly was located at around 70–75°N, 2 hPa with magnitude of 15–20 ms^{-1} on February 19. The easterly in high-latitudes was weakened after the reverse, and the westerly in low-latitudes became stronger than before (Figs. 2f and 3f). In the first two sudden warming events, however, the reverse of the zonal-mean zonal wind such as described above did not exist (not shown). From these analyses, it can be seen that the first two of the three sudden warmings were minor warming, and the third was a major warming.

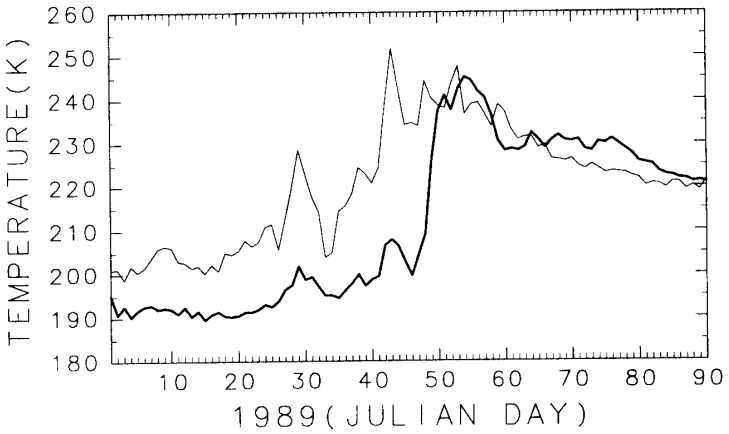

Fig. 1. Time evolution of temperature at 10 hPa (thin line) and 30 hPa (thick line) over the North Pole.

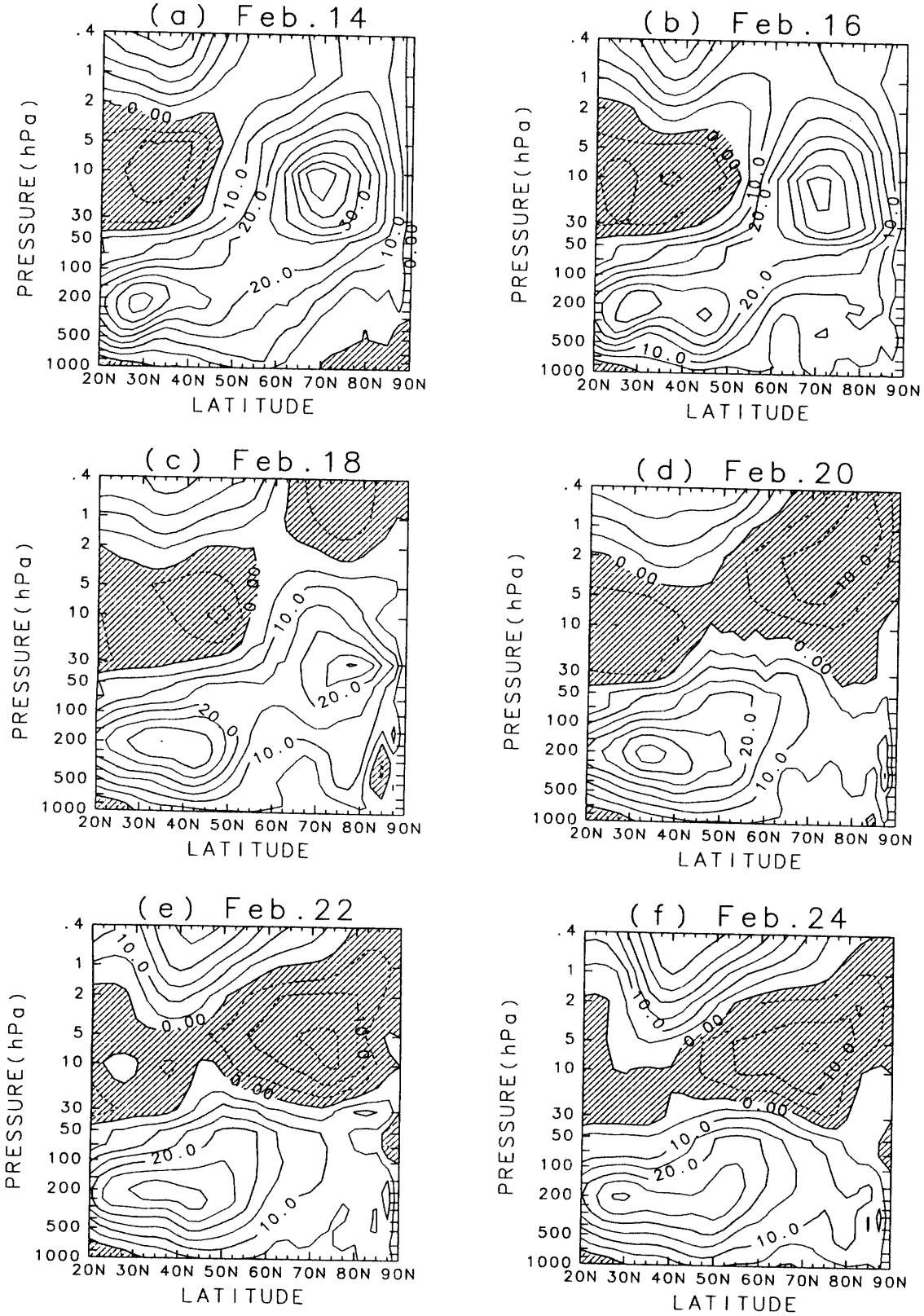

Fig. 2. Latitude-height sections of the zonal-mean zonal wind on February (a) 14, (b) 16, (c) 18, (d) 20, (e) 22, and (f) 24 in the Northern Hemisphere. Contour interval is 5 ms^{-1}. Negative values are hatched.

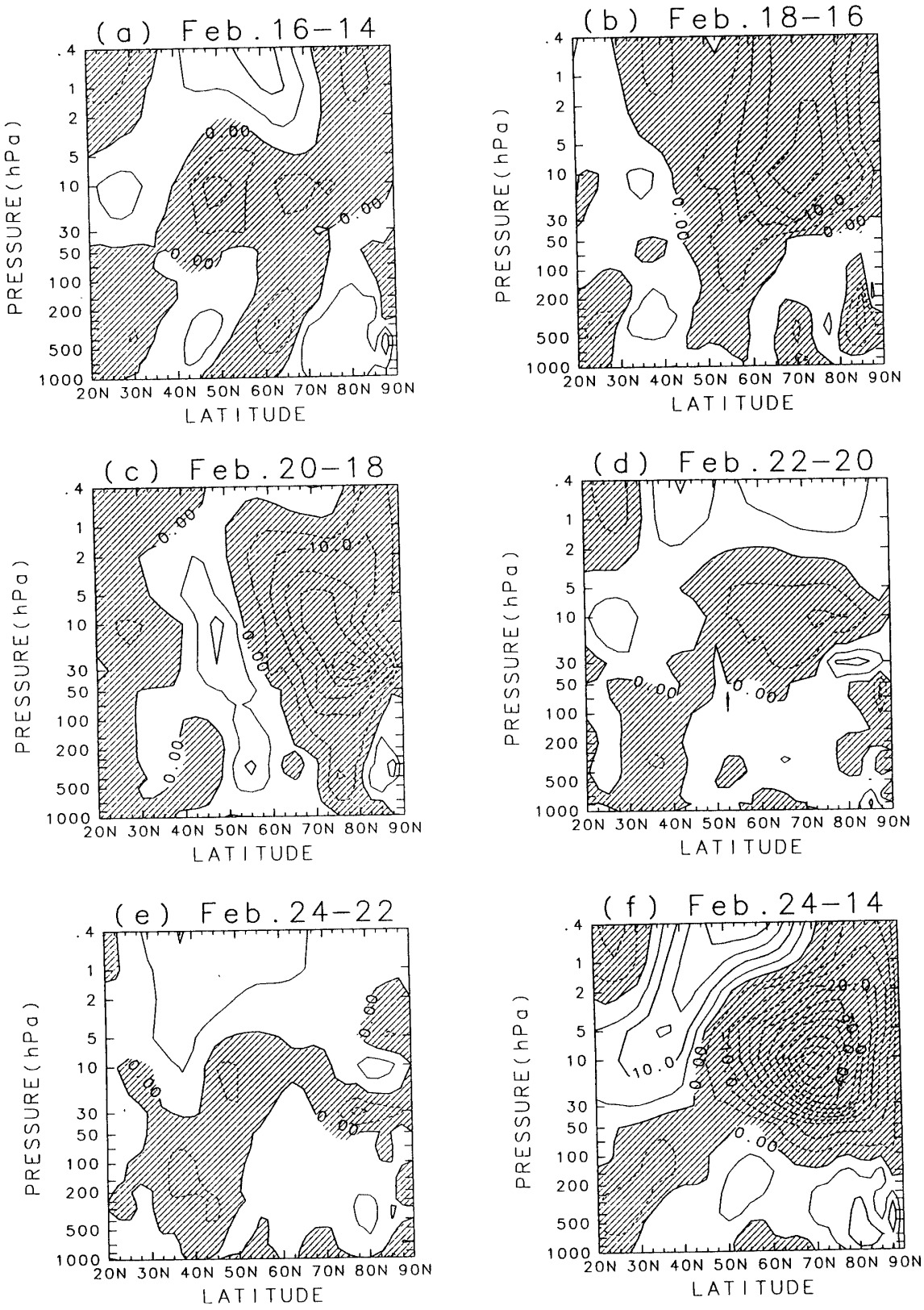

Fig. 3. Latitude-height sections of the change of the zonal-mean zonal wind for two days during the third stratospheric sudden warming. Contour interval is 5 ms^{-1}. Negative values are hatched.

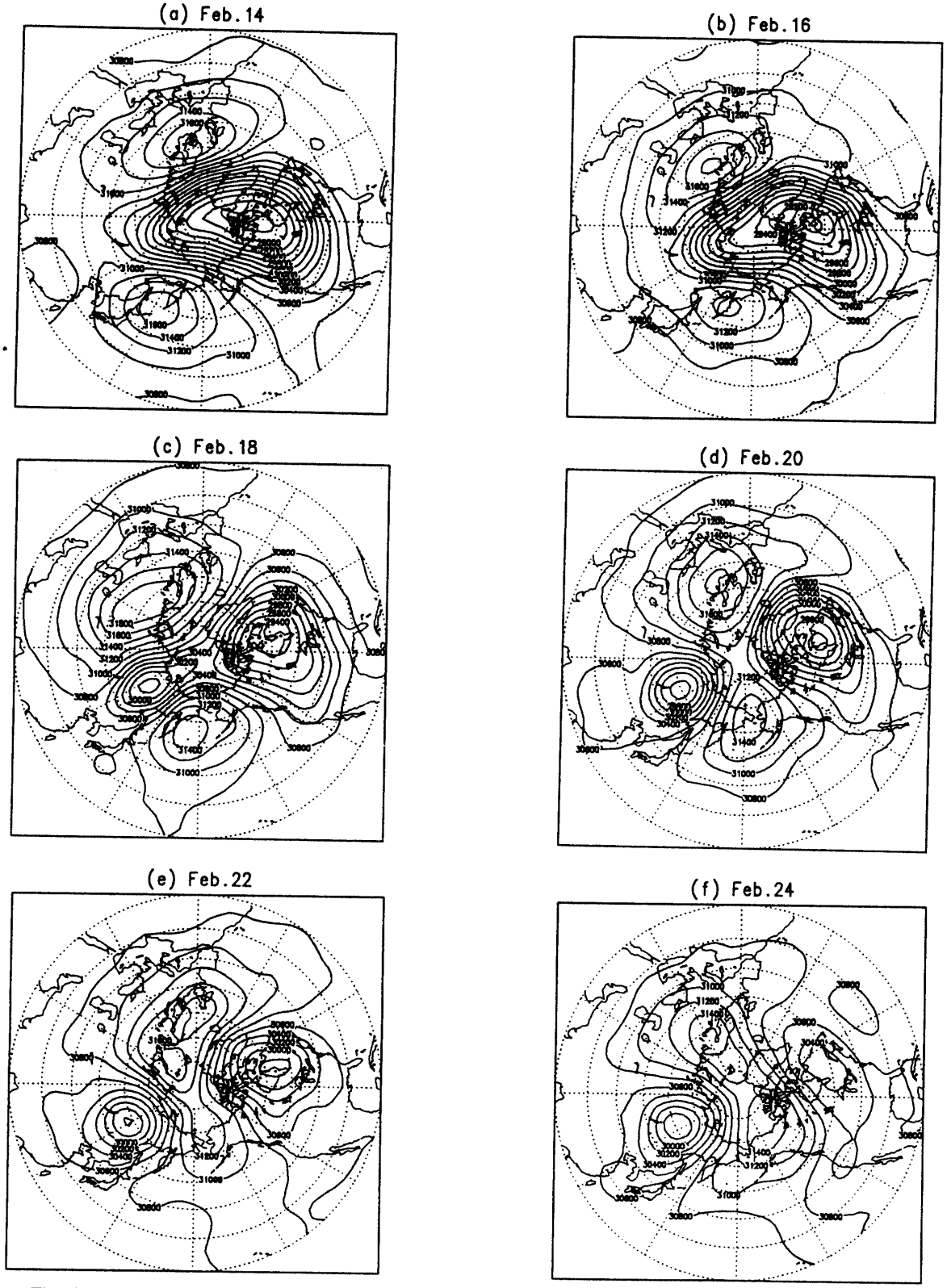

Fig. 4. Geopotential height maps at 10 hPa for the same days as in Fig. 2. Latitude circles are shown at 10° intervals, with the outermost circle at 20°N. Contour interval is 200 m.

Figure 4 shows the evolution of geopotential height fields at 10 hPa for the same days as in Fig. 2. On February 14, the polar vortex was elongated and was located near the pole. The Aleutian High and the high in the European sector are seen at around 155°E, 50°N and 10°E, 60°N, respectively. Associated with the sudden warming, the high in the European sector has strengthened and the polar vortex has weakened during the following few days (Figs. 3b and 3c). The strengthened high in the European sector moves poleward and eventually the polar vortex split into two cyclonic centers (Fig. 3d). Therefore the polar region was occupied by relatively warm air. But after the sudden warming, the high in the polar region was weakened (Figs. 3e and 3f), and the polar vortex recovered around March 1 (not shown). In this figure, it can be seen that the third warming event was a major warming of wavenumber-2.

3.2. E-P flux vectors and residual mean meridional circulation

Figure 5 shows the E-P cross sections, which are latitude-height sections containing the E-P flux vectors and the zonal force due to divergence of the E-P fluxes (see Section 2). In Fig. 5a, it is found that the E-P flux vectors which indicate the direction of planetary wave propagation moved strongly upward from the mid-latitude lower troposphere and played an important part in the deceleration of the mean flow in mid-latitudes of the upper stratosphere. At the same time, there was remarkable westerly wave forcing in high-latitudes of the upper stratosphere. After February 15, the magnitudes of the E-P flux vectors increased, and their directions turned more upward and poleward (Figs. 5b -5d). Intense easterly wave forcing is seen in high-latitudes of the upper stratosphere. The forcing extended to mid-latitudes by the change of the E-P flux vectors as mentioned above (Figs. 5b-5d). During this period, the easterly wave forcing reached a maximum of nearly 50 ms^{-1} day^{-1} at about 65°N, 10 hPa. Because the planetary wave from the lower troposphere was weakened after February 20, the easterly wave forcing was also weakened (Figs. 5e and 5f). The weak westerly wave forcing is shown in mid- and low-latitudes of the upper stratosphere (Figs. 5e and 5f). Wave forcing shown in Fig. 5 explains the observed wind change (Figs. 2 and 3) fairly well.

By wavenumber analysis, it is found that the E-P fluxes of wavenumber-1 and -2 played an important role in the easterly accelerations, but the wavenumber-2 pattern was especially dominant (not shown). Whereas E-P fluxes of wavenumber-1 contributed to the easterly accelerations in the upper stratosphere, those of wavenumber-2 contributed mainly to the easterly accelerations in the middle stratosphere (not shown). The E-P fluxes of higher wavenumbers did not contribute very much to the easterly accelerations in the stratosphere (not shown). These results confirm that the third sudden warming had a planetary wave of wavenumber-2.

Figure 6 shows the latitude-height sections of the residual mean meridional circulation for the same days as in Fig. 2. On February 14 (Fig. 6a), there were two counterclockwise circulations in the high-latitude stratosphere. In the mid-latitudes of the upper stratosphere, the meridional component of the residual circulation was generally poleward. On February 16 (Fig. 6b), the upper stratospheric counterclockwise circulation broke down. The meridional component of the residual circulation in the mid- and high-latitude upper stratosphere was generally poleward, and then a strong descent occurred in the polar region. The descent of the upper stratosphere became stronger than before and extended to the

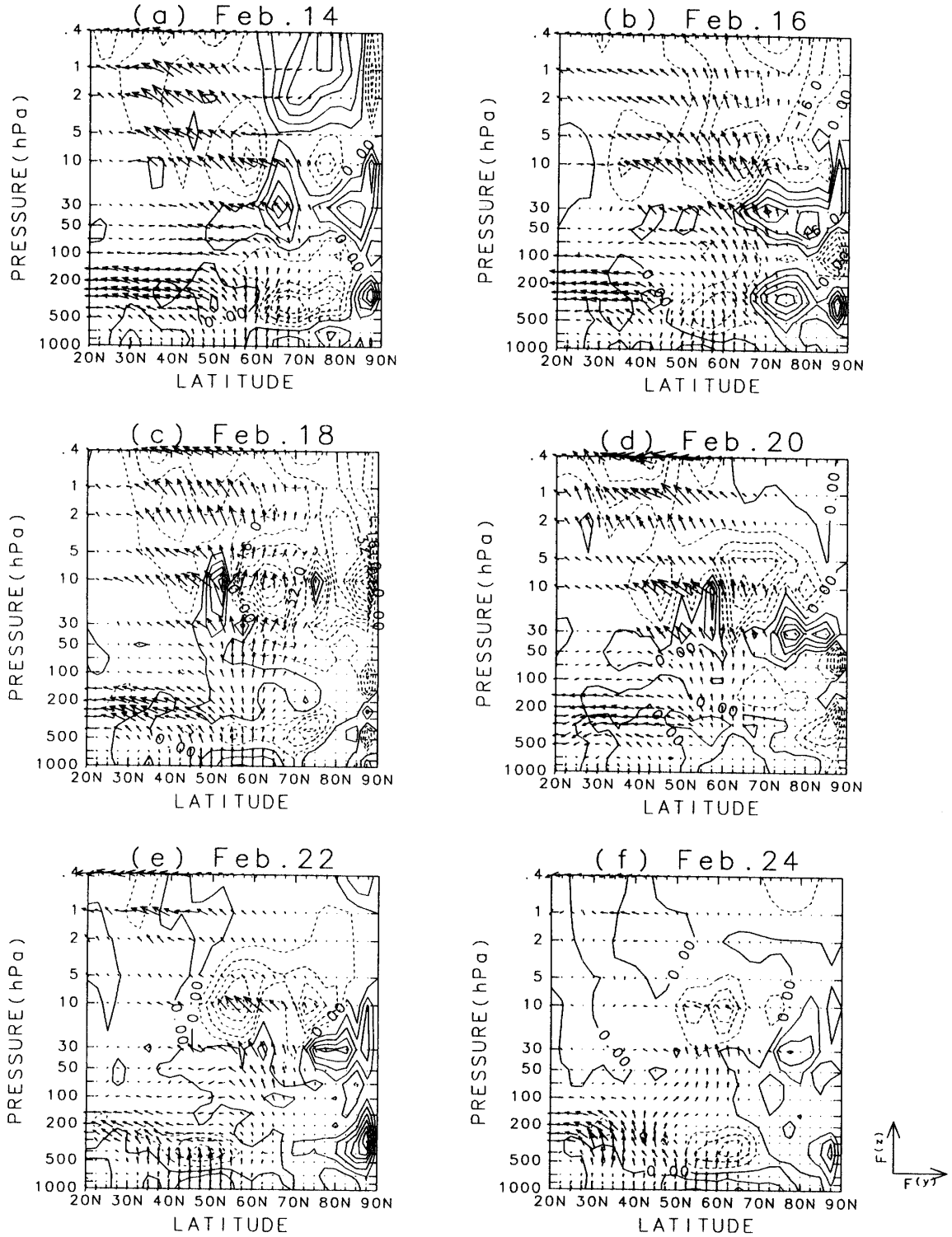

Fig. 5. Eliassen-Palm (E-P) cross sections in the Northern Hemisphere for the same days as in Fig. 2. Contours represent acceleration of the mean flow provided by the E-P fluxes, and contour interval is 8 ms^{-1} day^{-1}. The length of the E-P flux vectors is multiplied by the factor exp (z/H). Unit vectors over the meridional and vertical components of E-P flux vectors are 1×10^{17} $kgms^{-2}$ and 6.4×10^{14} $kgms^{-2}$, respectively.

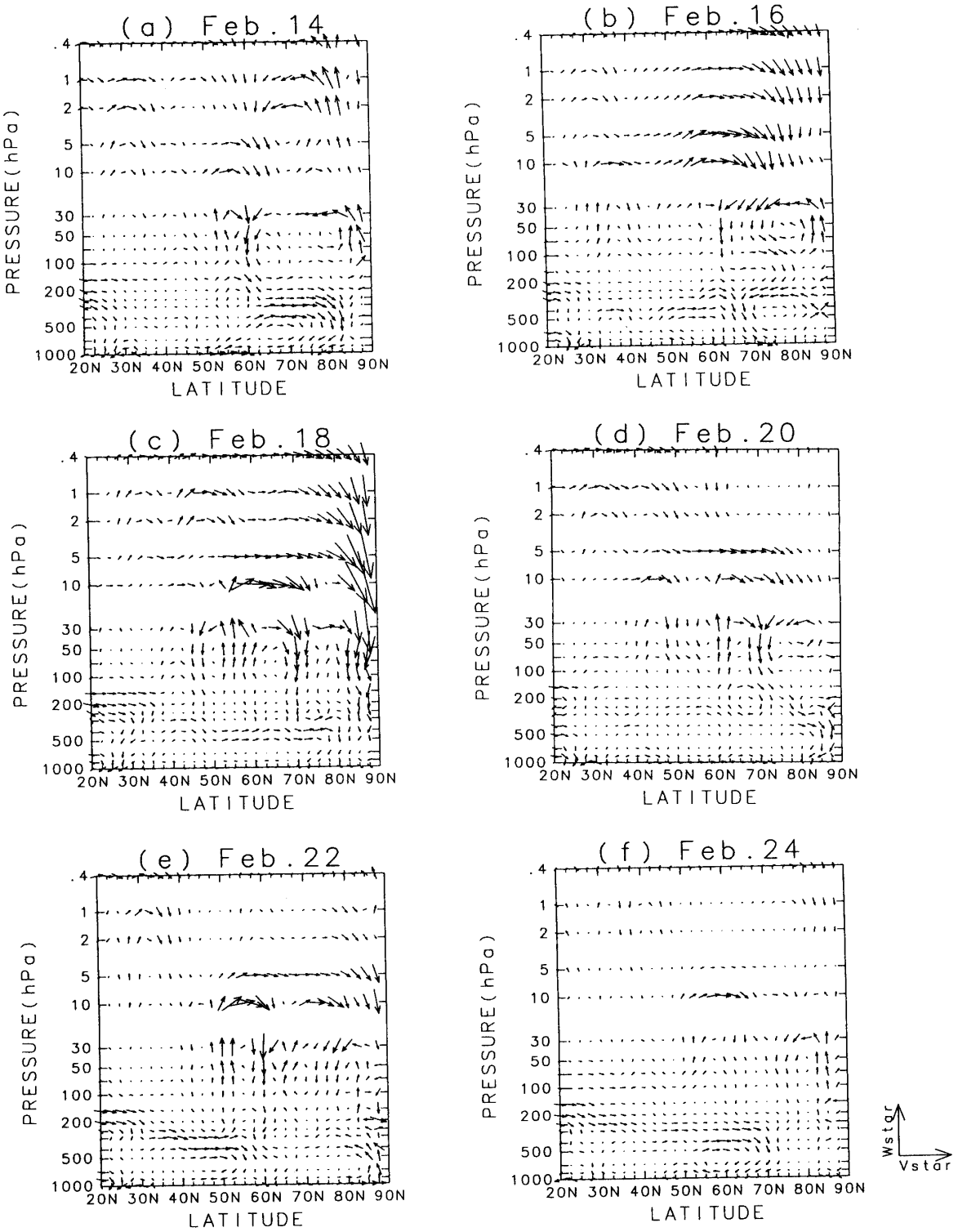

Fig. 6. Latitude-height sections of the residual mean meridional circulation in the Northern Hemisphere for the same days as in Fig. 2. Unit vectors of the meridional and vertical components are 10 ms^{-1} and 0.064 ms^{-1}, respectively.

troposphere (Fig. 6c). From Figs. 6a–6d, it can be seen that the intense warming from February 15 to February 20 in the northern polar stratosphere occurred by this strong descent. The ascent found somewhere in low-latitudes though the ascent was not well organized. After February 20, the descent weakened during the following few days, and the stratospheric residual circulation weakened quickly on February 24 (Figs. 6d–6f).

4. Relationship between the Stratospheric Sudden Warming and the AAM Variation

Figure 7a shows the time evolution of the AAM in the NH stratosphere (20–90°N, 100–0.4 hPa) with that of temperature at the North Pole, 30 hPa. In this figure, it is found that the AAM decreased largely by the stratospheric sudden warming events from January 22 to February 21. But it is noted that although the major warming took place abruptly around February 15–20, the AAM decreased gently during the 4 weeks before the major warming. After the major warming, the decrease of the AAM stopped, and the AAM increased. These characteristics of the AAM variation over the NH stratosphere are also shown in the global stratospheric AAM (see the thick line in Fig. 7b). During the 4 weeks, the enhanced planetary wave activity seems to have contributed to the reduction of the global stratospheric AAM. The global tropospheric AAM (see the middle thickness line in Fig. 7b) has also decreased before the major warming, and discussion about this aspect is made in Section 6.

The calculated total AAM, calculated tropospheric AAM, and LOD changes during January-March 1989 are shown in Fig. 8. Here the calculated total AAM and tropospheric AAM are shown in units of LOD (milliseconds (ms)) and estimated by applying equation, $\Delta LOD = 1.68\ \Delta AAM$, to the globally and vertically integrated AAM (the thin line and middle thickness line of Fig. 7b). In this equation, LOD in ms units and AAM in $10^{26}\,kgm^2s^{-1}$, and the constant 1.68 comes from the assumption of core-mantle decoupling (ROSEN and SALSTEIN, 1983; JADIN and YAMAZAKI, 1995). In Fig. 8, the mean difference between total AAM and LOD during the three months was removed. The calculated total AAM, calculated tropospheric AAM, and LOD gently decreased before the major warming and recovered after the major warming. The changes of the LOD correlated reasonably well with those of the calculated total AAM rather than the calculated tropospheric AAM from January to March. On January 22, with AAM maximum, and February 21, with AAM minimum, in the NH stratosphere (see the thick line in Fig. 7a), the calculated total AAM and LOD decreased as much as 0.29 and 0.14 ms, respectively. The contribution of the global stratospheric AAM to the decrease of the calculated total AAM is 48% (0.14 ms). If the beginning date is changed to January 26 when the calculated total AAM and LOD reached a maximum, the decreases of the calculated total AAM and LOD are 0.38 and 0.34 ms, respectively. The correlation is very good, and a contribution of the global stratospheric AAM to the decrease of the calculated total AAM is 37% (0.14 ms) for this period. It is shown that stratospheric winds contributed significantly to the total AAM during the warming events in 1989.

The decrease of the LOD related to the period of the stratospheric sudden warming is also seen in cases of other major warming (*e.g.*, major warmings of February 1979, February 1981, February 1984, December 1984, January 1987, and January 1991). We

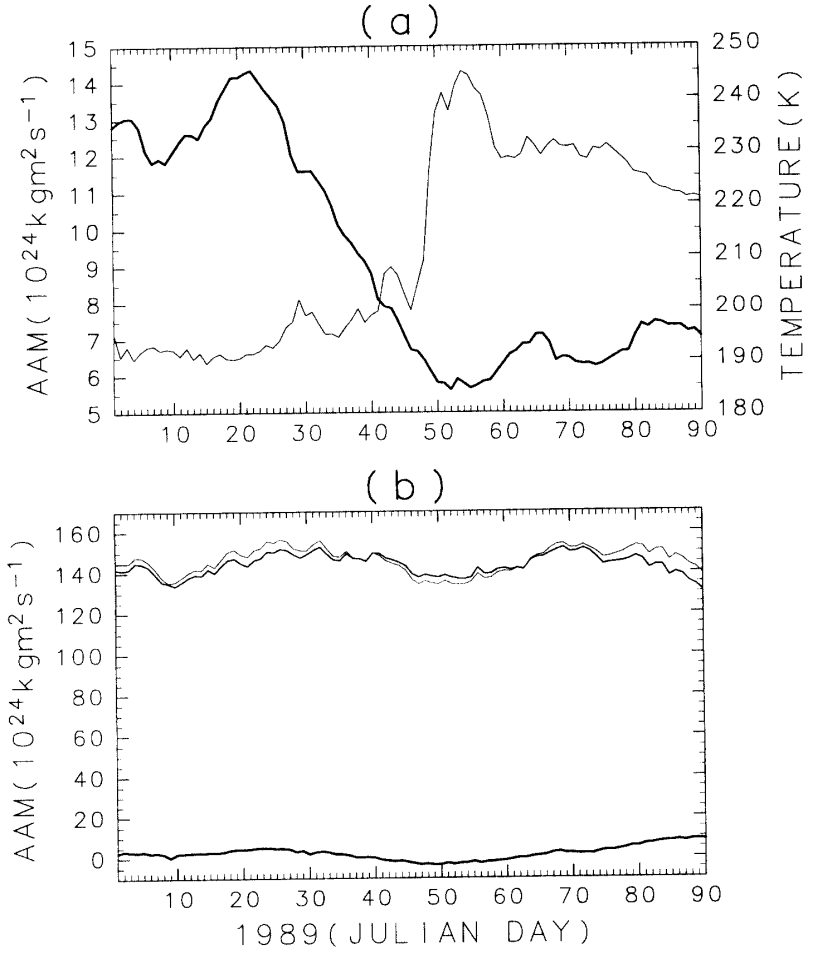

Fig. 7. (a) Time evolution of the AAM in the Northern Hemisphere stratosphere (20-90°N, 100-0.4 hPa: thick line) and temperature at the North Pole, 30 hPa (thin line). (b) Time evolution of the global (90°S-90°N) stratospheric AAM (100-0.4 hPa: thick line), tropospheric AAM (1000-100 hPa: middle thickness line), and total AAM (1000-0.4 hPa: thin line).

made a composite of 7 major warming means, including the 1989 case, and the result is shown in Fig. 9. Day 45 corresponds to the starting date of warmings. The relationships between AAM, LOD and stratospheric sudden warming such as the above described are also shown in this figure. These results suggest that not only the stratospheric AAM but also the tropospheric AAM decreases before the major warming and so does the LOD. This coherent variation between the tropospheric AAM and stratospheric AAM is unlikely to be caused by chance.

Figure 10 shows the absolute angular momentum ($\overline{m}$) multiplied by a cosine factor to investigate the regions and patterns of AAM changes for 1989 warming. Figures 10a and 10b show the latitude-height section over the difference of $\overline{m}\cos\phi$ between January 22 with AAM maximum and February 21 with AAM minimum in the NH stratosphere, while Figs. 10c and 10d show the same section in the period of the major warming, *i.e.*, from February 15 to February 20. In Figs. 10a and 10b, it can be seen that the AAM is decreased in the whole region of the NH stratosphere, in particular, the decrease is large

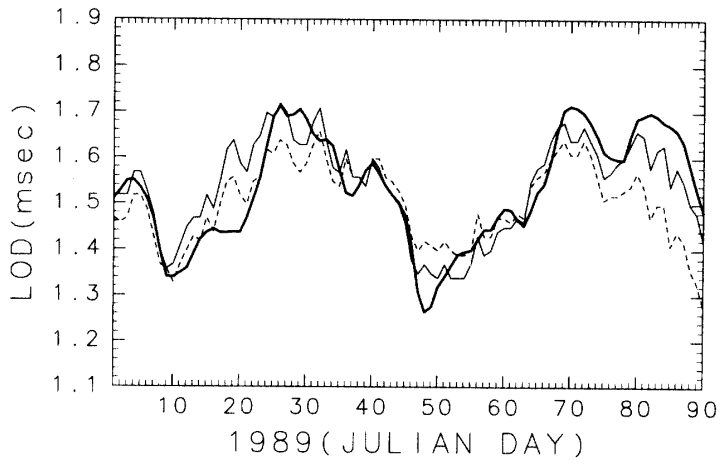

Fig. 8. Time evolution of the globally calculated total AAM (1000-0.4 hPa: thin solid line), calculated tropospheric AAM (1000-100 hPa: dashed line), and LOD changes (thick solid line).

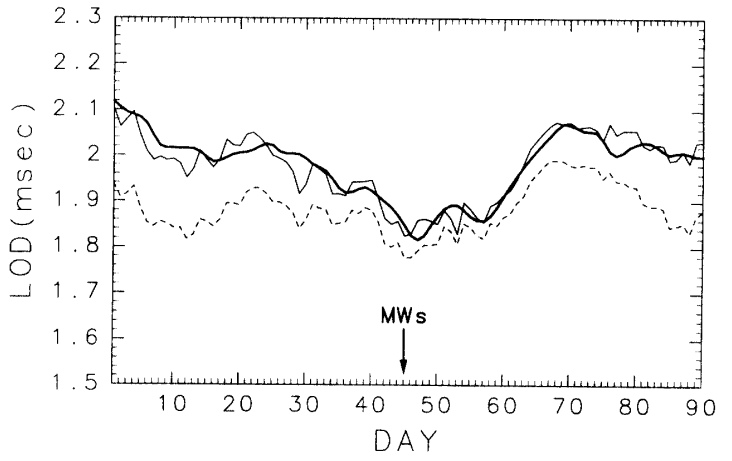

Fig. 9. As in Fig. 8, except for 7 case (major warmings of February 1979, February 1981, February 1984, December 1984, January 1987, February 1989, and January 1991) mean. Arrow (day 45) denotes the day that the major warmings (MWs) of 7 case were started.

in mid-latitudes of the stratosphere. The increase of the AAM in the Southern Hemisphere stratosphere is due to the regular seasonal change of zonal winds. In the cases in Figs. 10c and 10d, the AAM decreased at high-latitudes but increased at low-latitudes of the NH stratosphere. These results suggest that the northern stratospheric AAM in the period of the major warming does not vary very much from the viewpoint of the AAM budget. In other words, the importance of the major warming lies in the redistribution of the AAM within the stratosphere.

Figure 11 shows the latitude-time sections of $\overline{m}\cos\phi$ which are integrated vertically from 10 hPa to 100 hPa and from 0.4 hPa to 10 hPa, respectively. These figures assure that the decreasing of the AAM starts in the upper stratosphere of the northern hemispheric mid-latitudes (25-55°N) about 4 weeks before the major warming, and the increase of the

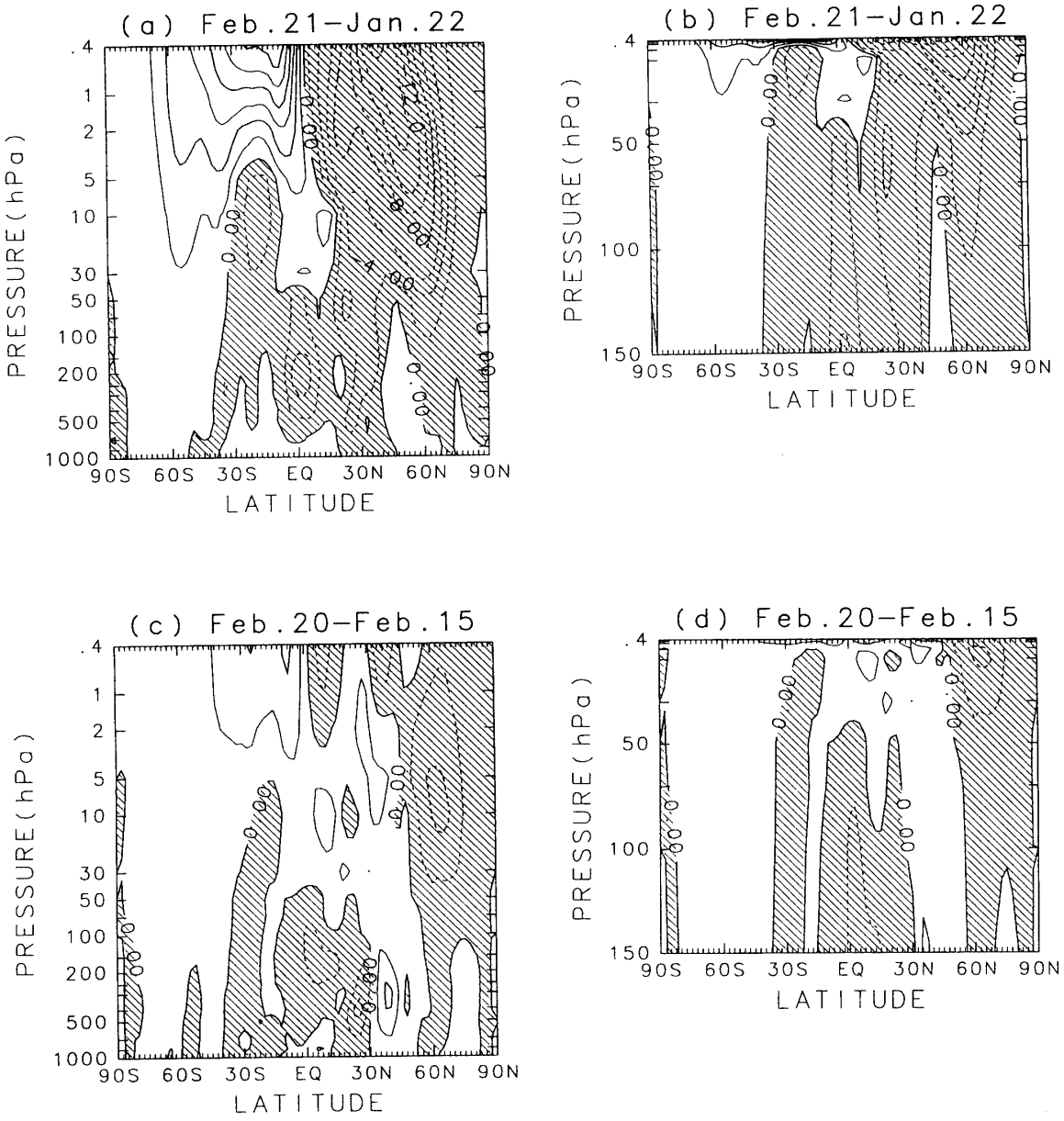

Fig. 10. Latitude-height sections of $\overline{m}\cos\phi$ variation between January 22 with AAM maximum and February 21 with AAM minimum in the Northern Hemisphere stratosphere ((a) log-pressure coordinates, (b) pressure coordinates) and in the period of the major warming ((c) log-pressure coordinates, (d) pressure coordinates). Negative values mean decreasing of the AAM and are hatched. Contour interval is 2×10^7 m^2 s^{-1}.

AAM after the major warming also starts from almost the same region.

5. AAM Budget in the NH Stratosphere

Figure 12 shows the time evolution of terms in eq. (12) and the observed AAM change (obtained by eq. (1)) over the region 20–90°N, 100–0.4 hPa. In this figure, it is found that eddy forcing (see the thick dashed line) and the observed AAM change (see the thick solid

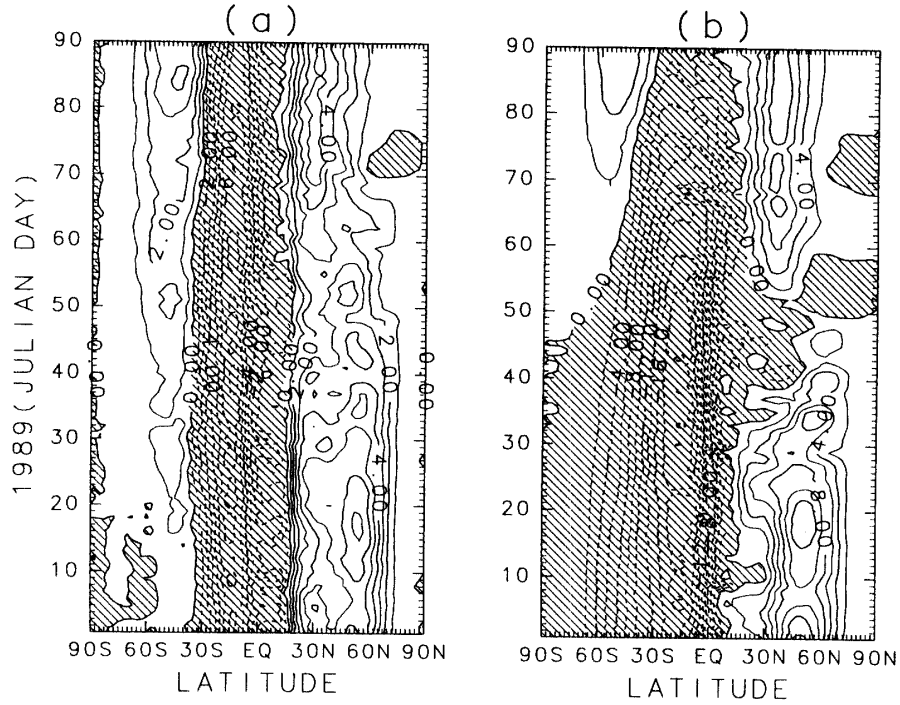

Fig. 11. Latitude-time sections of $\overline{m}\cos\phi$ integrated in vertical (a) from 10 hPa to 100 hPa and (b) from 0.4 hPa to 10 hPa. Negative values are hatched. Contour intervals in (a) and (b) are 1×10^{11} m^2 s^{-1} Pa and 2×10^{10} m^2 s^{-1} Pa, respectively.

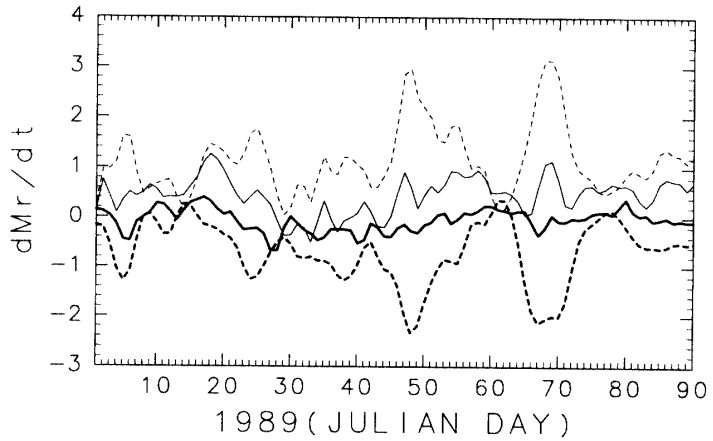

Fig. 12. Time evolution of the residual mean meridional circulation term (the sum of the first and second terms on the right-hand side: thin dashed line) in eq. (12), the eddy forcing term (the sum of the third and fourth terms on the right-hand side: thick dashed line) in eq. (12), and observed AAM change (thick solid line) over the region 20-90°N, 100-0.4 hPa. The thin solid line is the sum of the residual mean meridional circulation and eddy forcing terms. Units are 10^{24} kgm^2 s^{-1} day^{-1}.

line) terms are positively correlated, while the residual mean meridional circulation (see the thin dashed line) term is negatively correlated with the observed AAM change term. In other words, whereas eddy forcing plays an important role in the decrease of the AAM, the

residual mean meridional circulation contributes to the increase of the AAM. In comparing between the eddy forcing and the observed AAM change, it is noted that eddy forcing was enhanced gradually during the 4 weeks before the major warming, and it contributed to gradual decrease of the AAM. There can be seen several peaks of the eddy forcing in Fig. 12. From comparison between Fig. 12 and Fig. 1, it is found that a few days after significant enhancement of the eddy forcing, the stratospheric sudden warmings took place. For example, the eddy forcing reached the peak value on day 24 (January 24) and day 38 (February 7), and the first and second minor warmings occurred during days 26–29 (January 26–29) and days 40–43 (February 9–12), respectively. The strongest eddy forcing occurred around day 48 (February 17), and it caused the major warming during days 46–51 (February 15–20). In case of the enhancement of the eddy forcing around day 67 (March 8), a warming event was seen at high-latitudes of the lower stratosphere below 50 hPa. Here the residual mean meridional circulation and eddy forcing consist of the meridional components, the first and third terms on the right-hand side of eq. (12), and vertical components, the second and fourth terms on the right-hand side of eq. (12),

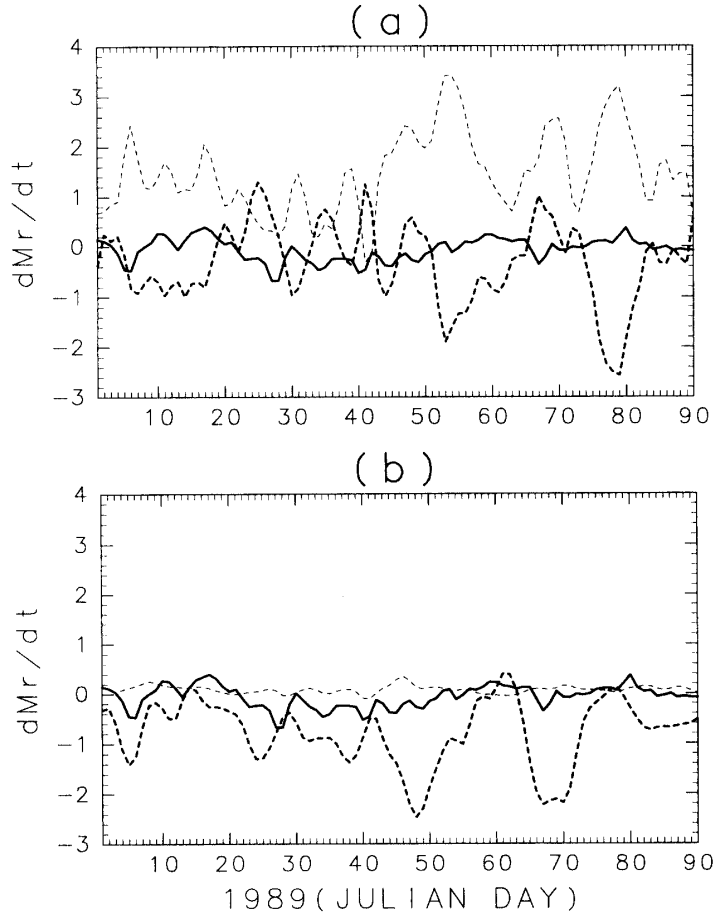

Fig. 13. Time evolution of the meridional (thin dashed lines) and vertical (thick dashed lines) components of (a) the residual mean meridional circulation and (b) the eddy forcing over the region 20–90°N, 100–0.4 hPa. Solid lines show the time evolution of observed AAM change over the same region. Units are 10^{24} *kgm*^{2} *s*$^{-1}$ *day*$^{-1}$.

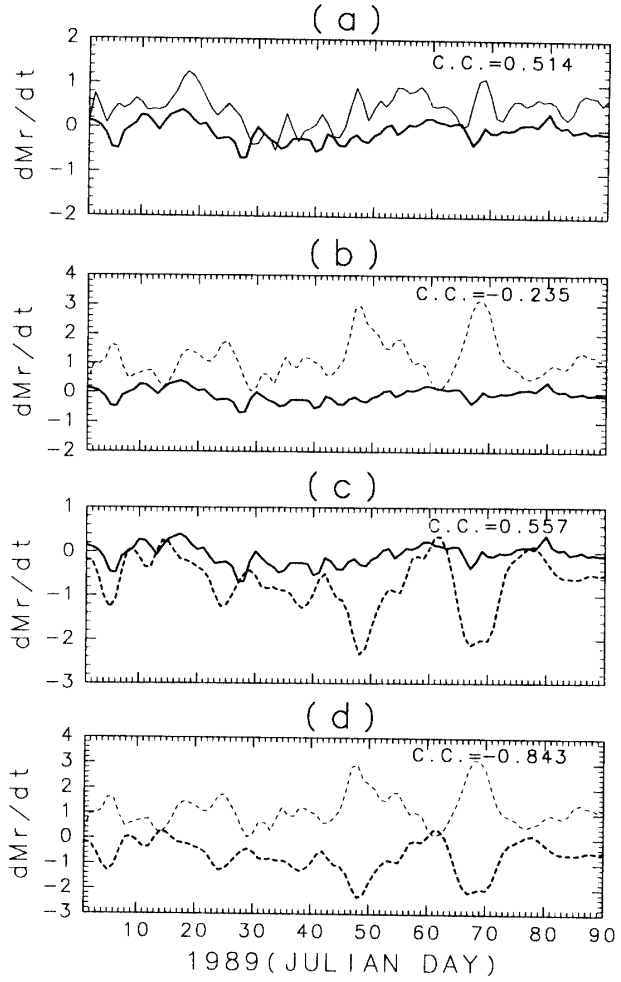

Fig. 14. Correlations over the terms that are shown in Fig. 12. (a) Correlation between observed AAM change (thick line) and time-variation of the AAM by the right-hand side of eq. (12) (thin line), (b) correlation between observed AAM change (solid line) and term of the residual mean meridional circulation (dashed line), (c) correlation between observed AAM change (solid line) and term of the eddy forcing (dashed line), and (d) correlation between term of the residual mean meridional circulation (thin line) and term of the eddy forcing (thick line). The ordinate units are 10^{24} kgm^2 s^{-1} day^{-1}.

respectively. In the AAM budget, the meridional component of the residual mean meridional circulation is more important than its vertical component (Fig. 13a), and the vertical component of the eddy forcing plays a larger part than the meridional component (Fig. 13b). Whereas the vertical component of the eddy forcing makes the AAM decrease, the meridional component of the residual mean meridional circulation makes the AAM increase by poleward transport of the large equatorial AAM and compensates for the decrease of the AAM. In other words, the vertical component of the eddy forcing and the meridional component of the residual mean meridional circulation are almost balanced from the viewpoint of AAM budget.

Figure 14 shows the correlations of the terms that are shown in Fig. 12. The 95% significance level is 0.210. The observed AAM change and time-variation of the AAM

calculated from the right-hand side of eq. (12) are reasonably well correlated (Fig. 14a). The correlation coefficients (c.c.) are 0.514. The observed AAM change has weak negative correlation with the residual mean meridional circulation term (Fig. 14b) but has strong positive correlation with the eddy forcing term (Fig. 14c). The residual mean meridional circulation term and the eddy forcing term show especially strong negative correlation (Fig. 14d). These figures confirm that the AAM is controlled by the eddy forcing from the troposphere, and the residual mean meridional circulation acts to compensate for the effect of eddy forcing. In Fig. 14a, although the correlation coefficients show strong positive correlations, some differences exist in variations of both lines. In general, the calculated AAM decrease is small compared with the observed AAM decrease. The fact that the calculated AAM decrease is smaller than the observed AAM decrease in Fig. 14a provides evidence that the westerly deceleration is not enough. If above the differences are not caused by the error in data or calculation, those must come from the neglect of $\overline{X}$ and/or unresolved eddies in $\nabla \cdot \mathbf{F}$ (see Section 2).

6. Summary and Remarks

The relationship between stratospheric sudden warmings and the AAM variation for January-March 1989 was examined. Using the angular momentum equation in the TEM formalism, the AAM budget was also investigated. Principal results obtained in this study can be summarized as follows:

1) In a series of stratospheric sudden warmings of 1989, the AAM of the NH stratosphere is largely decreased.
2) Although the major warming took place abruptly, the AAM decreased gently during the 4 weeks before the major warming. Such decreasing of the AAM is closely related to enhancement of the eddy forcing that started about 4 weeks before the major warming.
3) The AAM decreased in the whole region of the NH stratosphere. The decrease first occurred in mid-latitudes (25–55°N) of the upper stratosphere, and the increase of the AAM after the major warming also started from almost the same region.
4) During the major warming, the AAM decreased in high-latitudes but increased in low-latitudes of the NH stratosphere, and the total decreased slightly.
5) After the major warming, the decrease of the AAM stopped, and the AAM increased.
6) The decrease of the AAM by the major warming significantly contributed to the decrease of the global AAM and LOD, and the contribution of the global stratospheric AAM to decrease of the LOD is about 40–50%.
7) The eddy forcing is positively correlated with the time-variation of the AAM in the NH stratosphere, while the residual mean meridional circulation is negatively correlated with that. In other words, the eddy forcing decreases the AAM and the residual mean meridional circulation increases the AAM.
8) The vertical component of the eddy forcing and the meridional component of the residual mean meridional circulation play especially important roles in the AAM budget.

The relationships between stratospheric sudden warmings and the AAM such as described above are also seen in other major and final warmings that occurred from 1980 to 1994. In the major warmings of February 1981, December 1984, and January 1991, the

AAM of the NH stratosphere gradually decreased during the 4 weeks before the major warming and increased quickly after the warming (not shown). In the major warmings of February 1984 and January 1987, the AAM started decreasing about 5 weeks before the warming (not shown). In final warmings of March 1988 and 1993, the AAM, which decreased before the final warming did not increase after the warming (not shown). Here the final warming is defined as follows (YAMAZAKI, 1987): A significant temperature increase (*i.e.*, at least 20 degrees in zonal-mean in a period of a week or less) and circulation reversal to easterly are observed at any stratospheric level and this circulation remains after the event.

In this study, we found that northern stratospheric sudden warmings affect largely variations of the northern stratospheric AAM. However, the sudden warmings have almost no effect on variations of the southern stratospheric AAM. The global tropospheric AAM is also decreased (see Fig. 7b). The slight decrease of the northern tropospheric AAM in high-latitudes seems to be related to the northern stratospheric sudden warming (see Fig. 10). However, the main reduction of the global tropospheric AAM occurred in the tropics (see Fig. 10). Therefore the variation of the global tropospheric AAM is mainly related to the 40- to 50-day oscillation in the tropics (MADDEN, 1987; MAGAÑA, 1993). The reduction of the global tropospheric AAM prior to the stratospheric sudden warming is also shown in the composite analysis (Fig. 9). According to the present study, there seems to be a coherent variation of the 40- to 50-day oscillation and the stratospheric AAM. The physical mechanism which links to the tropical 40- to 50-day oscillation and the stratospheric AAM is not clear, though planetary wave activity in the mid-latitude troposphere is likely to be a key factor. It needs further study.

Acknowledgments

We are grateful to I. NAITO for providing the LOD data set, and to M. SHIOTANI for useful discussions. We also thank H. KANZAWA and an anonymous reviewer for helpful comments. The figures were produced by GFD-DENNOU Library and GrADS.

References

ANDREWS, D.G. and MCINTYRE, M.E. (1976): Planetary waves in horizontal and vertical shear: The generalized Eliassen-Palm relation and the mean zonal acceleration. J. Atmos. Sci., **33**, 2031–2048.

ANDREWS, D.G., HOLTON, J.R. and LEOVY, C.B. (1987): Middle Atmosphere Dynamics. Orlando, Academic Press, 489 p.

CHAO, B.F. (1989): Length-of-day variations caused by El Niño-Southern Oscillation and Quasi-Biennial Oscillation. Science, **243**, 923–925.

EDMON, H.J., Jr., HOSKINS, B.J. and MCINTYRE, M.E. (1980): Eliassen-Palm cross sections for the troposphere. J. Atmos. Sci., **37**, 2600–2616.

EUBANKS, T.M., STEPPE, J.A., DICKEY, J.O. and CALLAHAN, P.S. (1985): A spectral analysis of the Earth's angular momentum budget. J. Geophys. Res., **90**, 5385–5404.

GROSS, R.S. (1992): A combination of Earth orientation data. SPACE92. IERS Annual Report for 1992.

HOLTON, J.R., HAYNES, P.H., MCINTYRE, M.E., DOUGLASS, A.R., ROOD, R.B. and PFISTER, L. (1995): Stratosphere-troposphere exchange. Rev. Geophys., **33**, 403–439.

JADIN, E.A. and YAMAZAKI, K. (1995): Changes in the Earth's rotation and the atmospheric angular momentum on intra-annual and decadal time scales. Pap. Meteorol. Geophys., **45**, 113–120.

LANGLEY, R.B., KING, R.W., SHAPIRO, I.I., ROSEN, R.D. and SALSTEIN, D.A. (1981): A common fluctuation with a period near 50 days. Nature, **294**, 730–733.

MADDEN, R.A. (1987): Relationships between changes in the length of day and the 40- to 50-day oscillation in the tropics. J. Geophys. Res., **92**, 8391–8399.

MAGAÑA, V. (1993): The 40- and 50-day oscillations in atmospheric angular momentum at various latitudes. J. Geophys. Res., **98**, 10441–10450.

NAITO, I. (1988): The Earth's rotation and the atmosphere-ocean dynamics. Tenki, **35**, 291–311 (in Japanese).

NAITO, I. and KIKUCHI, N. (1992a): Atmospheric contributions to the irregular variations of the Earth's speed of rotation. Tenki, **39**, 17–22 (in Japanese).

NAITO, I. and KIKUCHI, N. (1992b): Atmospheric contributions to non-seasonal variations in the length of day. Geophys. Res. Lett., **19**, 1843–1846.

ONODERA, E. and NAITO, I. (1987): Has climate been correlative with LOD? A comment. Publ. Int. Latit. Obs. Mizusawa, **20**, 13–15.

PALMER, T.N. (1981): Diagnostic study of a wavenumber-2 stratospheric sudden warming in a transformed Eulerian-mean formalism. J. Atmos. Sci., **38**, 844–855.

RANDEL, W.J. (1987): The evaluation of winds from geopotential height data in the stratosphere. J. Atmos. Sci., **44**, 3097–3120.

ROSEN, R.D. and SALSTEIN, D.A. (1983): Variations in atmospheric angular momentum on global and regional scales and the length of day. J. Geophys. Res., **88**, 5451–5470.

ROSEN, R.D. and SALSTEIN, D.A. (1985): Contribution of stratospheric winds to annual and semiannual fluctuations in atmospheric angular momentum and the length of day. J. Geophys. Res., **90**, 8033–8041.

ROSEN, R.D., SALSTEIN, D.A., EUBANKS, T.M., DICKEY, J.O. and STEPPE, J.A. (1984): An El Niño signal in atmospheric angular momentum and Earth rotation. Science, **225**, 411–414.

YAMAZAKI, K. (1987): Observations of the stratospheric final warmings in the two hemispheres. J. Meteorol. Soc. Jpn., **65**, 51–66.

(Received October 21, 1996; Revised manuscript accepted June 6, 1997)